ENERGETIKA. 2008. T. 54. Nr. 4. P. 75–83

CFD modelling of turbulent confined jet mixing of incompressible viscous media

Andrei Chorny

A. V. Luikov Heat & Mass Transfer Institute, NAS of Belarus, 15, P. Brovka Street, 220072 Minsk, Belarus
E-mail: anchor@hmti.ac.by

The present article considers the RANS simulation results on the interaction between a turbulent axis-symetrical jet and a co-flow of incompressible media (Schmidt number Sc ≈ 1000) in a jet mixer. RANS modeling was made with the intent to predict flow phenomena in a co-axial jet mixer. Two different mixing regimes were analysed with and without a recirculation zone near a mixer wall. Verification of known and developed mixing models was based on comparing them with the available experimental data and LES results. Analysis of the numerical results was the evidence that the decay of the averaged mixture fraction and its variance by the developed RANS mixing model, considering the low-Reynolds number effects (the mechanical-to-scalar time ratio R and the turbulent Schmidt number Sc_σ in the transfer equation for the variance σ as a function of Re_t), is similar to the one by LES and from experiment.

Key words: jet mixer, turbulent mixing, confined jet, co-flow, mixture fraction

1. INTRODUCTION

At present, the problems of heat and mass transfer enhancement in a flow of different media have been the focus for constant attention of researchers in many countries [1–4]. This has been motivated by a necessity to solve a diversity of engineering tasks on technological processes encountered in power engineering, mechanical engineering, chemical and petroleum industries. Many of them cannot proceed without the mixing phenomenon [1, 2]. Fast and complete mixing of various fluids is often considered to be one of the factors governing the phenomena in combustion devices, engines, chemical reactors, burners, heat exchangers, and pumps. Geometrical parameters and mass flowrates as well as the thermal-physical properties of substances to be transferred predetermine the rate of mixing and its specific features.

In order to understand or model flows and processes, one has to predict the impact of various factors on the mixing of substances. In this article, special attention is paid to the influence of turbulence on flow dynamics and mixing.

The influence of turbulence on mixing is observed on all turbulence length and time scales of flow dynamics [1, 2]. On the one hand, the large-scale motion controls the rate of spreading of substances in the flow field. Information on this macromixing can be provided from the averaged substance concentration. On the other hand, when one considers mixing on the molecular level, the microscales are to be taken into account. A knowledge of micromixing requires detailed information on the statistics of concentration fluctuations.

A profound understanding of the physical mechanisms of mixing is possible only when the occurring phenomena are being analysed with the use of both the available experimental data and different mathematical models. The deepest insight into this understanding can be achieved invoking Computational Fluid Dynamics (CFD). Theoretical analysis of turbulent flows widely uses the approaches including mathematical models for statistical turbulence parameters with different closing. Among them are the RANS (Reynolds Averaged Navier-Stokes) [1, 3, 4] and the LES (Large Eddy Simulation) models [5] which adopt two averaging methods, i. e. the spatial averaging for LES and the time one for RANS. Unlike direct numerical simulation of turbulent flows [6], these approaches require less computer time and allow getting information on averaged turbulence characteristics depending on the initial mixing flow conditions.

In the past decades, numerous models for mixing in turbulent flows were developed [1–5]. The difference between these models lies in the manner how the macromixing and micromixing are related to the turbulence. The existing models do not always provide accurate computations of scalar fields, e. g., the averaged concentration field in the turbulent flow. This means that we are not yet able to model correctly macromixing and micromixing in the turbulent flow. This is so for several reasons. One of the reasons is the lack of a fundamental understanding of mixing in the turbulent flow. Another reason is the lack of experimental and numerical data on turbulent mixing for different geometries used for the validation of mathematical models [1–4]. The proposed suitable models are validated by verifying the results obtained by these models, and then the correct model assumptions can be chosen. The experimental measurements and numerical simulations used for this purpose have earlier been extended mainly to mixing in homogeneous turbulent flows [1, 3, 4, 7]. Turbulent mixing in shear flows is being extensively investigated at present as in many applications turbulence is inhomogeneous, and thus

data on mixing in turbulent shear flows are of particular interest [1–4, 8]. A jet flow is one of the most widespread types of shear flows in feasible problems. The turbulent jet mixing is of significance in solving the problem on obtaining a uniform distribution of transferred substances and a homogeneous mixture in injection facilities where jets develop [2]. A distinctive feature of the results of the present article is investigation of the impact of turbulence on the mixing of incompressible viscous fluids in confined jet flows [8]. The objective of this article is to develop mathematical tools based on the CFD modelling of turbulent confined jets of incompressible viscous media and to elucidate the main factors governing the mixing of media to be transferred within different flow regimes as required by the inlet hydrodynamic and geometrical parameters of an axis-symmetrical jet mixer.

2. SPECIFIC FEATURES OF TURBULENT MIXING IN JET MIXER

It is known [9] that in the axis-symmetrical mixer two topologically different flow regimes are possible: 1) when a recirculation zone develops near the channel walls (*r*-mode); 2) when such a zone does not develop (*j*-mode). Its development can be explained by a simple model for a jet interacting with co-flow. A jet issuing from the inner tube injects some co-flow fluid amount that is proportional to velocity difference in the jet and in the flow. If the jet volume injected by the jet per unit time is larger than the fluid flowrate in the co-flow, then the flow pattern is reversed, the co-flow separates at the mixer walls, and the recirculation zone develops. Simple estimates by this model yield the inequality $1 + Q < D/d$, whose compliance means that the mixer flow is accompanied by developing a recirculation zone. The experimental findings support the validity of this rule (see, e. g., [8–11]).

In [8], it is shown that the recirculation zone near the cylindrical channel walls brings about a difference in the turbulent characteristics decay and affects the mixing rate of the passive admixture to be transferred by the flow. For the ratios of flowrates ($Q = 1.3$ and 5) and diameters ($D/d = 5$), a homogeneous mixture in the *r*-mode is formed by four diameters earlier than in the *j*-mode [8]. For $Q = 1.3$, a recirculation zone develops starting with the distance $x/D > 0.1$, its center is located between the cross-sections $2.1 < x/D < 2.6$, and the boundary of its decay lies immediately behind the cross-section $x/D = 3.1$. The influence of the developed recirculation zone on the mixing may be analysed by calculating the radius-averaged mixture fraction f_{av}. Just the macromixing rate for both mixing regimes can be first estimated by varying the normalized mixture fraction value f_N along the mixer (Fig. 1) where in the initial cross-section the quantity $f_0 = f_{av}$ for both regimes is the same, $f_\infty = 1 / (Q + 1)$ is the value of f_{av} at complete mixing. Fig. 1 shows a similar mixing only at a small distance ($x/D < 0.6$). Downstream, the macromixing occurs much faster in the *r*-mode regime and is close to the completion stage, starting with $x/D = 3.1$ (f_N approaches its asymptotic value $f_N = 1$), whereas in the *j*-mode regime such a state is seen only at $x/D = 9.1$.

The quantity r_j is responsible for the jet transverse size and within the *j*-mode regime points to a probable position of the mixing layer formed at the jet and co-flow interface. Within the *r*-mode regime, the integral parameter r_j already does not convey the information exclusively on the transverse size of the turbulent jet since the jet and co-flow interaction is affected by the recirculation zone near the mixer walls. This fact illustrates both a sharp growth of r_j for $x/D < 2.1$ and the obtaining of the asymptotic value of 0.5 (Fig. 1), thus indicating a considerable admixture content over the entire mixer cross-section. Such specific features of the recirculation zone influence the turbulent characteristic variations and must be taken into account when constructing effective statistical models. That is why in this article RANS mixing models were developed and verified with an intent to predict flow phenomena in a coaxial jet mixer.

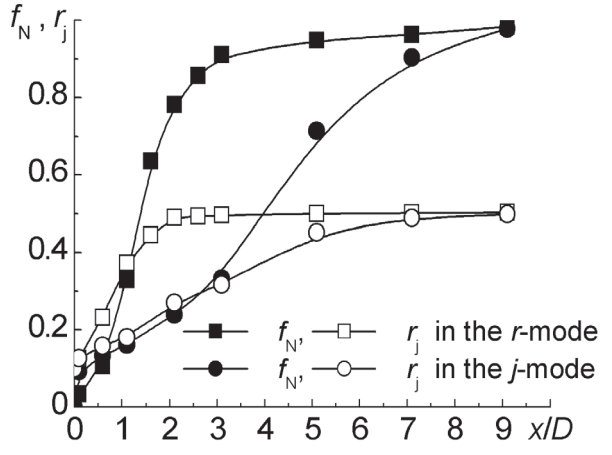

Fig. 1. Integral parameters f_N and r_j for both mixing regimes where, $f_N = (f_{av} - f_0)/(f_\infty - f_0)$, $f_{av} = \frac{1}{24}\int_0^{1/2} r^2 \overline{f}\, dr$ and $r_j = \sqrt{3\int_0^{1/2} r^2 \overline{f}\, dr \Big/ \int_0^{1/2} \overline{f}\, dr}$ (the quantities *r* and r_j are dimensionalized to *D*)

3. TURBULENT MIXING MODELLING

3.1. Velocity field modelling

3.1.1. The continuity equation and the Reynolds averaged Navier–Stokes (RANS) equations

The continuity and the Reynolds averaged Navier–Stokes (RANS) equations are

$$\frac{\partial \overline{u}_i}{\partial x_i} = 0, \quad \frac{\partial \overline{u}_i}{\partial t} + \frac{\partial \overline{u}_i \overline{u}_i}{\partial x_j} = -\frac{1}{\rho}\frac{\partial \overline{p}}{\partial x_i} + \frac{\partial}{\partial x_i}\left[\nu\left(\frac{\partial \overline{u}_i}{\partial x_j} + \frac{\partial \overline{u}_j}{\partial x_i}\right) - \overline{u_i' u_j'}\right]$$

Here $\overline{u_i' u_j'}$ is the turbulent stress tensor. In the majority of engineering models for turbulent flows, this tensor is assigned using the Boussinesq hypothesis [4]. In this case, the transfer equations for turbulent characteristics are closed by determining unknown correlations through averaged flow parameters. The Boussinesq hypothesis enables writing the turbulent stress tensor through the deformation rate tensor of the averaged velocity invoking the turbulent viscosity ν_t by analogy with the molecular viscosity ν.

3.1.2. Turbulence model

Turbulence is characterized by two parameters – turbulence kinetic energy *k* and its dissipation rate ε. The standard *k*–ε model

is adopted for their predicting. In this model, assuming developed local-isotropic turbulence, the Kolmogorov–Prandtl formula $\nu_t = C_\mu k^2 / \varepsilon$ is used to determine the turbulent viscosity ν_t. Here C_μ is a model constant.

In many engineering predictions of turbulent flows, the standard values of the empirical constants C_μ, σ_k, σ_ε, $C_{\varepsilon 1}$, $C_{\varepsilon 2}$ [4] are chosen for the standard k–ε model by comparing the predicted results and the available experimental data on a wall jet and a mixing layer of an incompressible fluid. It is known [12] that for axis-symmetrical free jets the standard turbulence k–ε model with such a set of constants yields an overestimated result on the rate of jet expansion and decay. Therefore, to improve the accuracy of such a model, one uses the equation for the dissipation rate ε modified by adding a term based on the concept of eddy stretching. A somewhat different approach is associated with varying the constants $C_{\varepsilon 1}$ and $C_{\varepsilon 2}$ in the terms of the equation responsible for the amplification and attenuation of kinetic energy dissipation [12]. As the ratio $C_{\varepsilon 1} / C_{\varepsilon 2}$ is increased, the expansion rate of a round jet decreases. Increasing only $C_{\varepsilon 1}$ also delays the decay of the jet which in this case occupies the elongated and narrowed flow regions. In [13], the C_μ and $C_{\varepsilon 2}$ choice depends on the jet velocity decay and the expansion radius [14]:

$$C_\mu = 0.09–0.04\xi;\ C_{\varepsilon 2} = 1.92–0.0667\xi;\ \xi = \left| \frac{R_j}{2(U_{ax} - U_D)} \left(\frac{\partial U_{ax}}{\partial x} - \left| \frac{\partial U_{ax}}{\partial x} \right| \right) \right|^{0.2}$$

Here R_j is the jet expansion radius, U_{ax} is the axial averaged velocity. Assuming the linear x dependence of R_j and the inverse x dependence of U_{ax} [15] allows taking $C_\mu = 0.06$ and $C_{\varepsilon 2} = 1.87$.

In [16], a set of the constants invoked into the free turbulent jet study is adopted to verify the turbulence k–ε model for a round turbulent jet when mixed with the co-flow bounded by the cylindrical channel walls. The predictions of the longitudinal component of the averaged velocity U and the kinetic energy k by the standard k–ε model with different sets of constants show that k–ε model modification with $C_\mu = 0.06$ and $C_{\varepsilon 2} = 1.87$ is the best among the considered ones from the viewpoint of the accuracy of predicting the kinetic energy k for both mixing regimes. In this case, for the j-mode regime, the variations of this turbulent parameter are in a rather complete agreement with the experimental data [8].

3.2. Passive admixture mixing modelling

To analyse the mixing process in the jet mixer, the variations of the first two statistical moments – the averaged value $\bar{f}$ and the variance of the mixture fraction – are considered. The averaged value $\bar{f}$ is a characteristic of large-scale transfer of substances dissolved in the fluid – a rate of attaining macromixing. The mixing up to molecular scales (fine-grained mixing – micromixing) is determined by the fluctuation decay of transferred substance concentration in the flow and is associated with varying the mixture fraction variance σ^2 due to the scalar dissipation rate ε_S.

The equations for $\bar{f}$ and σ^2 in the mixing model are usually written on the gradient diffusion assumption similar to the Boussinesq hypothesis for velocity parameters [4]. This assumption predetermines the turbulent scalar flux vector through an averaged scalar value when the turbulent diffusivity D_t identical to the molecular one is introduced. The value D_t is expressed in terms of the turbulent viscosity ν_t and the turbulent Schmidt number Sc_t ($D_t = \nu_t / Sc_t$). So, the transfer equations for $\bar{f}$ and σ^2 are obtained in the form

$$\frac{\partial \overline{f}}{\partial t} + \frac{\partial \overline{u}_j \overline{f}}{\partial x_j} = \frac{\partial}{\partial x_j} \left[\left(\frac{\nu}{Sc} + \frac{\nu_t}{Sc_t} \right) \frac{\partial \overline{f}}{\partial x_j} \right],$$

$$\frac{\partial \sigma^2}{\partial t} + \frac{\partial u_j \sigma^2}{\partial x_j} = \frac{\partial}{\partial x_j} \left[\left(\frac{\nu}{Sc} + \frac{\nu_t}{Sc_\sigma} \right) \frac{\partial \sigma^2}{\partial x_j} \right] + 2 \frac{\nu_t}{Sc_t} \left(\frac{\partial f}{\partial x_j} \right)^2 - \varepsilon_S .$$

Here, Sc_σ is the turbulent Schmidt number in the equation for the variance, which is in its sense similar to Sc_t in the equation for the averaged mixture fraction.

As for the equation for σ^2, one should know how to determine the scalar dissipation rate ε_S. For this purpose, a widespread model for ε_S is the algebraic one based on varying the mechanical-to-scalar time ratio $R = \tau_t / \tau_S$ between time scales of turbulent fluctuations of the velocity $\tau_t = k / \varepsilon$ and the concentration $\tau_S = \sigma^2 / \varepsilon_S$ (scalar mixing time) [4]. Here $\varepsilon_S = \sigma^2 / \tau_S = R\, \sigma^2 / \tau_t$.

3.2.1. Mixing models

In modern studies of axis-symmetrical round jets, the turbulent Schmidt numbers Sc_t and Sc_σ are assumed to be constant and equal to 0.7. Assuming that R is constant (usually $R = 2$) enables one to write a widespread mixing model at $R = 2$, $Sc_t = Sc_\sigma = 0.7$ [4] (hereinafter MM1) valid for a fully developed scalar spectrum, i. e. the mixing is suggested to occur on all length and time scales. Moreover, dissipation should be at equilibrium with the generation of concentration fluctuations on large scales. Also, the velocity and concentration fluctuations should be generated in a similar manner and depend on the same physical mechanisms. Such dynamic properties are realized mainly for gas flows. Therefore, the MM1 has found wide use in the fluid with the molecular Schmidt numbers of the order of unity. However, it is known [17] that in the general case for a defined value of Sc the mechanical-to-scalar time ratio R is the function of a local Reynolds number Re_t calculated through a rms velocity fluctuation $u' = \sqrt{2k/3}$ and a turbulence length scale l_t. Therefore, at $Sc >> 1$, the MM1 overestimates the micromixing rate. R as a function of Re_t is determined by the energy scalar spectrum form [17]. In turbulent incompressible fluid flows with high Sc numbers (in our case at $Sc = 1000$), the dissipation and generation of concentration fluctuations are determined by their variations at three stages characteristic of inertia-convective, viscous-convective, and viscous-diffusive ranges of the energy scalar spectrum.

The work [3] contains the Corrsin model for the scalar dissipation time scale that takes into account the presence of the viscous-convective range and permits writing $R = (2 + 1 / Sc) / (3 + \mathrm{Re}_t^{-1/2} \ln \mathrm{Sc})$ as a function of both Sc and Re_t. The multi-time-scale $\bar{f}$ –σ^2 model [3] represents a model constructed with regard to the specific features of fluid mixing with high Sc. In our work, R is determined by its polynomial Re_t dependence valid for fluid with $Sc = 1000$ and involving the low-Reynolds-number effects in the mixing model [17]: $R = \sum_{n=0}^{6} a_n \left(\log(\mathrm{Re}_t) \right)^n$ where $a_0 = 0.4093$, $a_1 = 0.6015, a_2 = 0.5851, a_3 = 0.09472, a_4 = -0.3903, a_5 = 0.1461$,

$a_6 = -0.01604$. Hereinafter, such a model at fixed $Sc_t = Sc_\sigma = 0.7$ is named the MM2.

As our further computations have shown, to analyse the $\bar{f}$ variations throughout the flow it is quite enough to assume the constant value of the turbulent Schmidt number $Sc_t = 0.7$ that has been used in the RANS modelling. The low-Reynolds-number effects are especially reflected in the variations of σ^2 being a characteristic of a small-scale transfer of substances in the flow field. Taking into account R as a function of Re_t makes it necessary to consider the local Sc_σ variations in the equation for variance. Similarity theory shows that the unknown dependence on $k, \varepsilon, \sigma^2, \tau_t, \tau_S$ can be written involving two dimensionless parameters [e. g., 18]:

$$q_1 = \frac{\nu_t \varepsilon_S^2}{Sc_\sigma (\sigma^2)^2 \varepsilon} = \frac{\nu_t}{Sc_\sigma} \frac{1}{\tau_S^2 \varepsilon}, \qquad q_2 = \frac{k\varepsilon_S}{\varepsilon\sigma^2} = \frac{\tau_t}{\tau_S} = R.$$

As a result, the turbulent diffusion in the σ^2 equation can be written as $\nu_t / Sc_\sigma = \varepsilon\tau_S^2 G(R)$, where $G(R)$ is an unknown R dependence. Out of possible means of assigning $G(R)$, consider $G(R) = C_S C_\mu \frac{\tau_t \tau_S}{\tau_S^2} = C_S C_\mu R$ (C_S is the model constant) that follows from the $\sqrt{\tau_t \tau_S}$ assumption as a mixed time scale of diffusion energy [19]. Then, the regard to the definition for $\nu_t = C_\mu k^2 / \varepsilon$ allows writing the dependence for $Sc_\sigma = \frac{\nu_t}{C_\mu C_S \tau_S^2 \varepsilon R} = \frac{R}{C_S}$ where, as our further computations have shown, $C_S \approx 1 / Sc_t$. Hereinafter, the mixing model with $Sc_t = 0.7$, the polynomial Re_t dependence of R and $Sc_\sigma = R / C_s$ is named the MM3.

3.3. Boundary conditions and model realization

RANS modelling was performed, assuming the axis-symmetrical steady incompressible fluid flow in the jet mixer. Because of the symmetry condition, a 2D rectangular domain 0.6 m long (12 mixer diameters) and 0.025 m wide (a half mixer diameter) was considered in the longitudinal direction from the jet exit and in the radial direction from the mixer axis. In the initial section of the computational domain (plane of jet issuing), the initial profiles were determined for all desired functions. It is known that for developed turbulent flow in a tube with a diameter d, the longitudinal velocity profile is described by the power law $U = U_{\max} (1 - 2r / d)^{1/n}$ and the radial velocity equals 0, where $U_{\max}$ is the maximum value of the longitudinal velocity in the cross-section (usually on the tube axis). In [15], the value of n is equal to 7. An alternative method of assigning the initial profiles is associated with their estimation from the available experimental distributions. In the present work, the modelling was performed when both the power-law profile and the constant longitudinal velocity were predetermined at the jet exit. From the available experimental data [8], the longitudinal velocity profile was developed at the co-flow entrance. The radial velocity was equal to zero.

The profiles of the turbulent characteristics of the jet and the co-flow were found from the relations for the kinetic energy $k = 1.5 Tu^2 U^2$ and for its dissipation rate $\varepsilon = C_\mu^{3/4} k^{3/2} / l_t$. The turbulence intensity $Tu = u' / U$ was estimated as $Tu = 0.16\, \mathrm{Re}_H^{-1/8}$. The initial length scale of the turbulence l_t was assigned by the relation $l_t = 0.07 D_H$, where D_H is the hydraulic diameter, based on which the Reynolds number Re_H was calculated. For the jet issuing $D_H = d$ and for the co-flow incoming $D_H = D - d$. According to the definition, the averaged value $\bar{f}$ is equal to 1 at the jet exit and takes the value 0 at the co-flow entrance, and the variance σ^2 equals zero. At the symmetry axis, the axial boundary conditions are set for unknown functions. At the walls, the velocity no-slip condition is set, and the fluxes of the functions $\bar{f}$, σ^2 are equal to zero. The equations for the k–ε model are valid for the developed locally isotropic turbulence. Near the wall, the boundary layer exists, for which this assumption is violated, i. e. $\mathrm{Re}_t << 1$. Therefore, the wall function method involving the wall logarithmic law was applied for assigning turbulent characteristics near the wall.

Computations were made on a non-uniform 800×60 space grid with the cells crowded together near the jet exit, the flow axis, and in the wall region. The transfer equations for desired functions were solved by FLUENT 6.2 with a second-order discretisation scheme and refining the pressure by the SIMPLE algorithm of Patankar and Spalding. A number of iterations were determined by reaching the accuracy of 10^{-6} for all functions. For realization of the mixing models, the FLUENT UDS module was used.

4. RESULTS

The mixture fraction f served as the parameter of the passive admixture mixing and was determined as the ratio of the local concentration c of the passive admixture dissolved in the jet to its concentration c_0 at the jet exit in the initial cross-section of the mixer: $f = c/c_0$. Then $f = 1$ at the jet exit and $f = 0$ at the co-flow entrance in the initial mixer cross section. Figure 2 illustrates the variations of the averaged value of the mixture fraction $f_{ax} = \bar{f}(x, 0)$ along the mixer axis for the two mixing regimes obtained using different turbulence models in comparison with experiment [8].

As follows from Fig. 2, the region of the constant-concentration admixture is seen near the turbulent jet exit up to $x/D = 1$ for both mixing regimes. However, the results obtained by different RANS models and the LES model with DGM SGS [20] overestimate the length of this region as much as twice. Then an intensive mixing occurs, which is followed by the formation of a homogeneous mixture. This is seen in attaining f_{ax} of the asymptotic quantity f_∞ (complete mixing) in the predictions by all models. Within the r-mode (Fig. 2, b) such attainment by all models is observed at some advanced rate as compared to the experimental data, and is approximately by four diameters earlier than within the j-mode (Fig. 2, a). The f_{ax} prediction along the mixer axis by the standard k–ε model with $C_\mu = 0.06$ and $C_{\varepsilon 2} = 1.87$ with the power-law velocity profile at the turbulent jet exit yields the results identical to the predictions by the Reynolds stress model and by LES with the DMM SGS model for both mixing regimes [20] (Fig. 2).

Figure 3 presents variations of the relative variance σ / f_{ax} of the mixture fraction. The numerical results obtained using different mixing models are compared with the available experiment [8] and the predictions by LES with two SGS models – DMM and DGM [20].

For the considered mixing regimes, MM1 and MM2 yield the values of σ variations along the mixer axis (Fig. 3) over-

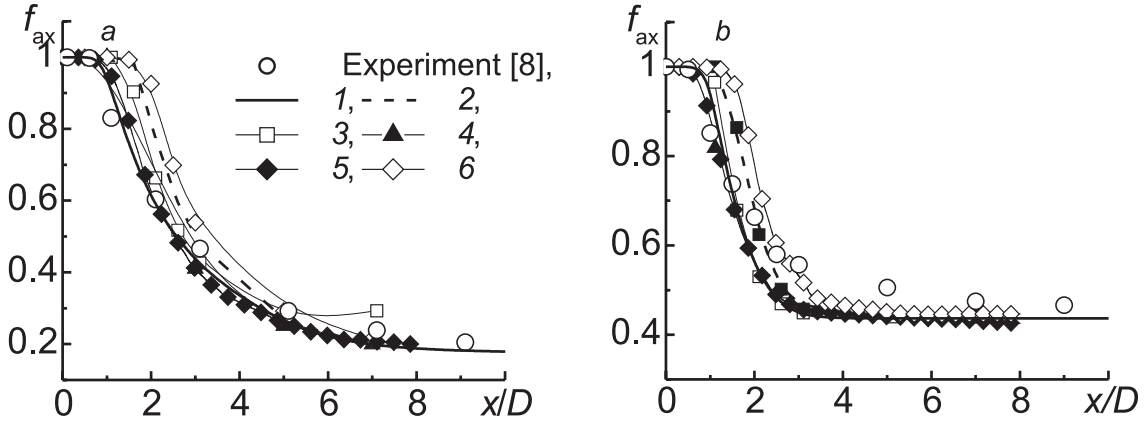

Fig. 2. Averaged mixture fraction along the mixer axis for two mixing regimes (*a* – *j*-mode, *b* – *r*-mode): *1* – standard *k*–ε model with $C_\mu = 0.06$ and $C_{\varepsilon 2} = 1.87$; *2* – *k*–ε model [20]; *3* – SST *k*–ω model [20]; *4* – Reynolds stress model [20]; *5* – LES model with DMM SGS and *6* – LES model with DGM SGS [20]

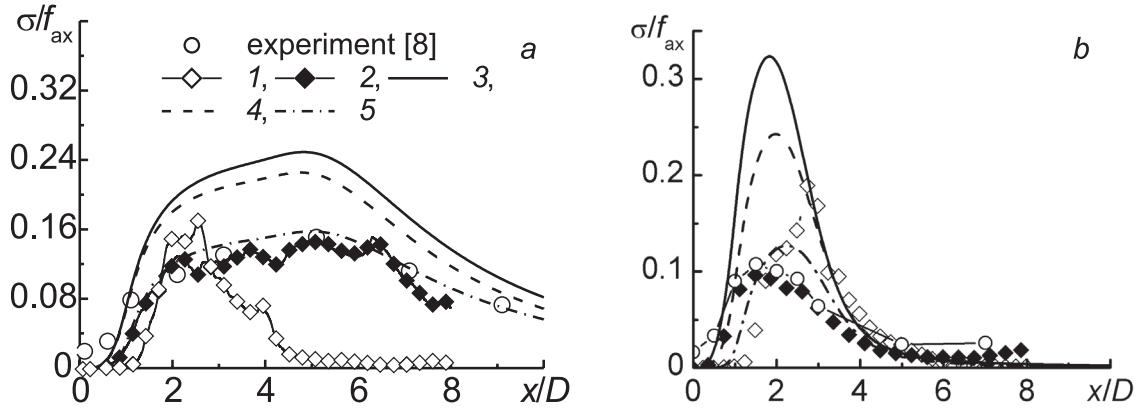

Fig. 3. Variance σ along the mixer axis for two regimes (*a* – *j*-mode, *b* – *r*-mode): *1* – LES with DGM, *2* – LES with DMM [20], *3* – MM1, *4* – MM2, *5* – MM3

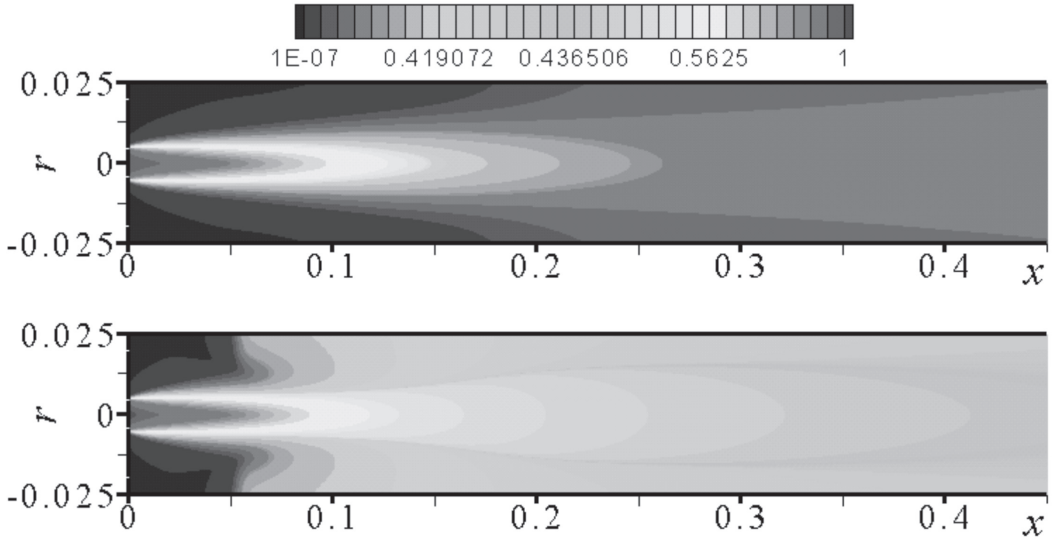

Fig. 4. Mixture fraction distributions within *j*-mode (*a*) and *r*-mode (*b*)

estimated with reference to experiment and LES. Yet in this case, the general tendency remains: first the level of relative fluctuations increases due to both the dynamic mixing of the jet and the fluid entrained from the co-flow at the expense of large-scale convective transfer and turbulent diffusion (macromixing), and then the fluctuation decays due to the intensive dissipation process. At the same time, the regard to the low-Reynolds effects in the MM3 causes the variance variations

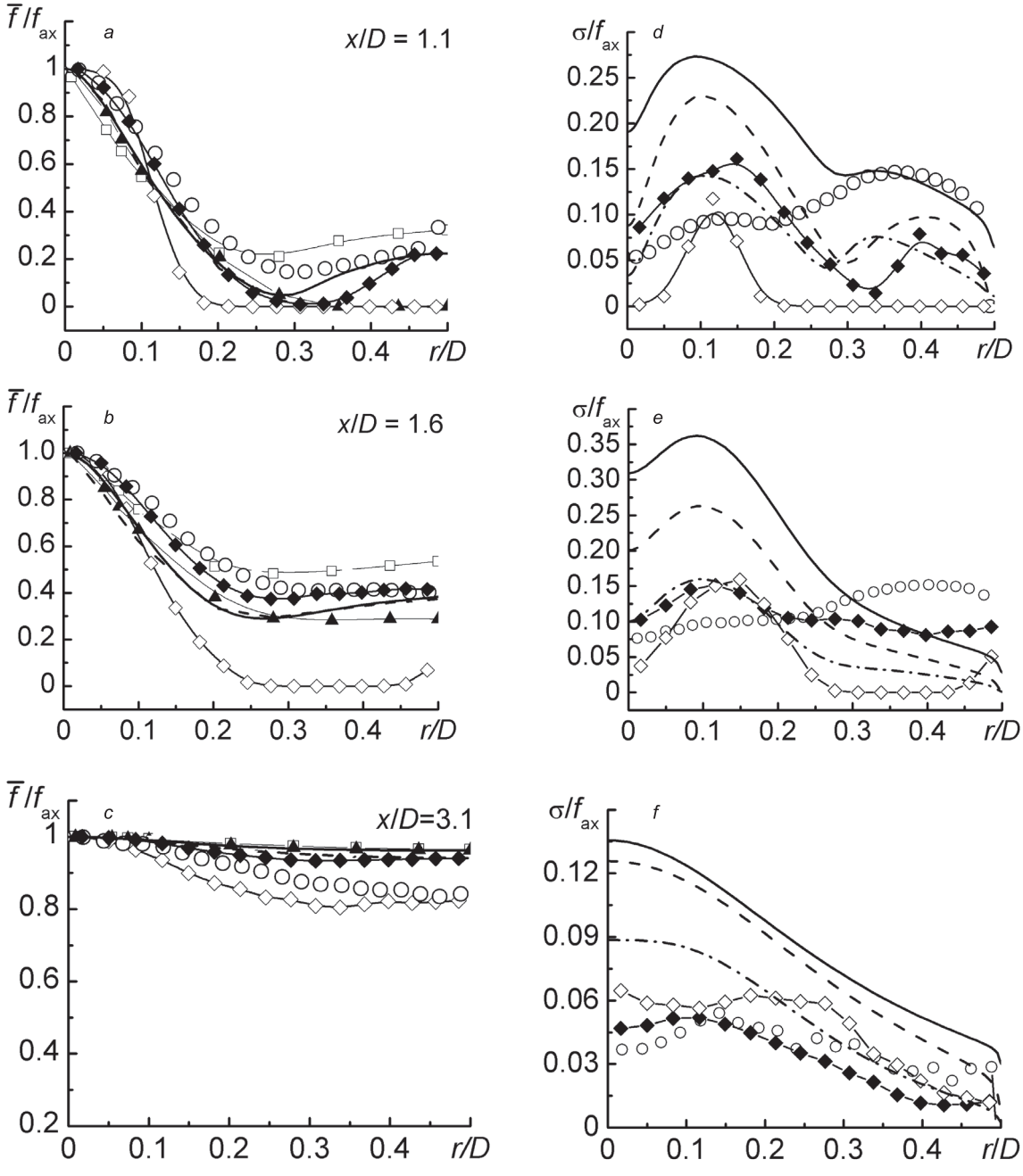

Fig. 5. Averaged mixture fraction $\bar{f}$ (*a*–*c*) and its variance σ (*d*–*f*) over the mixer cross-section at different distances from the jet exit in the *r*-mode. Notations of computation results are as in Fig. 2 for $\bar{f}$ and as in Fig. 3 for σ

to be consistent with experiment and LES with the DMM SGS model for the *j*-mode and provides a more qualitative agreement within the *r*-mode.

The $\bar{f}$ distributions obtained by the standard k–ε model with $C_\mu = 0.06$ and $C_{\varepsilon 2} = 1.87$ and the transfer equation for the averaged mixture fraction $\bar{f}$ (Fig. 4 a, b) demonstrate a qualitative difference in the structure of admixture transfer for two mixing regimes, which appears because of a recirculation zone developing within the *r*-mode regime. The $\bar{f}$ distribution points to the fact that starting from the distance $x/D \geq 0.6$, a recirculation zone appears and the passive admixture concentration near the mixer walls increases. This fact is seen in the form of the profile $\bar{f}(x, r)$ over the mixer cross-section (Fig. 5 a, b). The backflow transfer of the passive admixture along the mixer walls in the direction opposite to the jet motion increases the passive admixture concentration in this region. Hence $\bar{f}$ grows. Downstream, the $\bar{f}$ profile expands faster than against the averaged velocity profile [8, 16]. As a result, a nearly quasi-homogeneous composition of a mixture is formed over the mixer cross-section already at $x/D \geq 3.1$ (Fig. 5 c, f) and much earlier than a uniform distribution of the averaged velocity ($x/D > 5.1$) [8, 16]. Based on the results presented in Fig. 5, analysis of the profiles of the averaged mixture fraction and its rms fluctuations indicates that the recirculation zone starts behind $x/D = 0.1$, decays to $x/D = 5.1$, and its center is located within the distance range $2.1 < x/D < 2.6$.

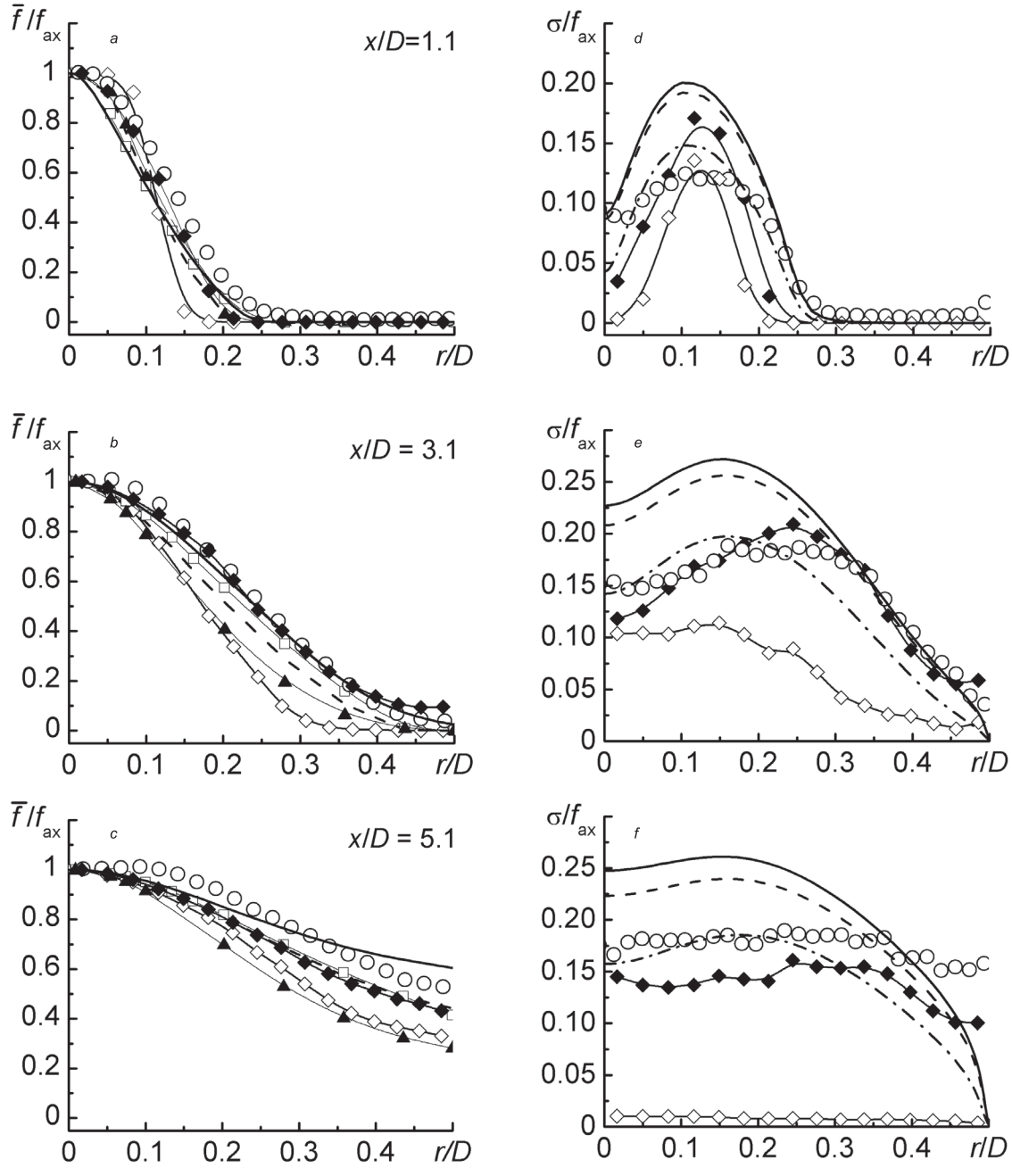

Fig. 6. Averaged mixture fraction $\bar{f}$ (*a–c*) and its variance σ (*d–f*) over the mixer cross-section at different distances from the jet exit in the *j*-mode. Notations as in Fig. 5

In the absence of the recirculation zone within the *j*-mode, the mixing proceeds more slowly. As shown in [8], the quasi-uniform distribution of the admixture starts only at $x/D = 9.1$. The $\bar{f}$ profile (Fig. 6 a–c) expands much faster than the averaged velocity one [4, 10]. The reason can be only a high intermittence level in the shear layer at the jet boundary. The σ/f_{ax} profiles (Fig. 6 d–f) are also wider about their maximum values as compared to those of the velocity fluctuations, and expand much faster than the latter [8, 16]. The values of the mixture fraction variance in the macromixing region ($x/D \geq 5.1$) are close to those of the velocity fluctuations, whereas at $x/D = 9.1$, as shown in [8], they are almost three times larger than those obtained in the *r*-mode mixing regime.

Figures 5 and 6 compare the profile of the averaged value $\bar{f}(x, r)$ with the calculation results obtained by different computational approaches. All models other than LES with the DGM SGS model [20], show a similar agreement with experiment [8]. A difference is present in the description of the backflow region for which the *k*–ε model with $C_{\mu} = 0.06$ and $C_{\varepsilon 2} = 1.87$ and LES with the DMM SGS model [20] yield a result more consistent with experiment [8].

The profile change of the variance σ (Figs. 5, 6 d–f) obtained by the mixing models illustrates the overestimated values of the intensity of scalar fluctuations in comparison with the available experimental data [8]. Nevertheless, both the LES [20] and the RANS models suggest that the position of the local maxima of the profile at the jet and co-flow interface within both regimes (Fig. 5 d–f, 6 d–f) is identical to the one found in experiment [8]. Similarly to the result on the σ decay (Fig. 3), the MM1 and the MM2 give a worse prediction of this quantity than against the

MM3 and LES with the DMM SGS model [20]. Analysis of the transfer equation for the variance σ^2 in both models indicates that the difference first of results from the used approximations of the scalar dissipation rate with regard to the low-Reynolds number effects. In the MM1, the time scale of the scalar dissipation rate is determined by the energy of only the developed inertia-convective part of the spectrum, whereas in the MM2 and in the MM3 also by the viscous-diffusive mixing rate.

5. CONCLUSIONS

The RANS modelling of mixing of a turbulent jet with a co-flow of incompressible viscous media (Schmidt number $Sc \approx 1000$) in an axis-symmetrical jet mixer is made employing the standard turbulence k–ε model and different mixing models.

To solve the problem of the passive admixture transfer in an axis-symmetrical mixer, two mixing regimes – with and without a recirculation zone near the mixer wall – are considered. Such specificity of the presence of two regimes makes a qualitative difference in the flow structure, which is evident from the fact that developing the recirculation zone near the mixer wall requires less time for a complete mixing. The result obtained in the present study is supported by the analysis of the predicted averaged mixture fraction and its variance both along the mixer axis and in the mixer cross-sections at different distances from the turbulent jet issue in comparison with LES [20] and experiment [8].

The averaged mixture fraction calculated by the standard turbulence k–ε model with the constants $C_\mu = 0.06$, $C_{\varepsilon 2} = 1.87$ and the power-law velocity profile at the turbulent jet exit yields the result similar to the one predicted by the Reynolds stress model and by LES for both mixing regimes [20]. However, the widespread mixing model with $R = 2$ overestimates the mixture fraction variance with respect to experiment and LES. The obtained numerical results have shown that the changes in the averaged mixture fraction and its variance observed by the developed RANS mixing model considering the low-Reynolds number effects (the mechanical-to-scalar time ratio R and the turbulent Schmidt number Sc_σ in the transfer equation for the variance σ as a function of Re_t) are similar to the ones obtained by LES with the DMM SGS model [20] and to experimental data [8].

Further studies will involve the development of LES and RANS models to account for the unsteady phenomena in confined jet flows with chemical reacting.

ACKNOWLEDGEMENT

The author would like to express his gratitude to the Belarusian Republican Foundation of Fundamental Research (T08P-101) and World Federation of Scientists for supporting this work.

Received 10 November 2008
Accepted 17 December 2008

References

1. Brodkey R. S. (ed.). Turbulence in mixing operations. London and N. Y.: Academic Press, 1975. P. 339.
2. Schetz J. A. Injection and mixing in turbulent flow. N. Y.: American Institute of Aeronautics and Astronautics, 1980. 200 p.
3. Baldyga J., Bourne J. R. Turbulent mixing and chemical reactions. N. Y.: Wiley & Sons, 1999.
4. Fox R. Computational models for turbulent reacting flows. Cambridge: Cambridge University Press, 2003.
5. Ferziger J. H. Large eddy simulations: its role in turbulence research // Dwoyer D. L., Hussaini M. Y., Voigt R. G. (eds.). Theoretical approaches in turbulence. N. Y.: Springer–Verlag, 1987. P. 51–72.
6. Moin P., Mahesh K. Direct numerical simulation: a tool in turbulence research // Ann. Rev. Fluid Mech. 1998. Vol. 30. P. 539–578.
7. Eswaran V., Pope S. B. Direct numerical simulation of the turbulent scalar mixing using of a passive scalar // Phys. Fluids. 1988. Vol. 31. No. 3. P. 506–520.
8. Zhdanov V. L., Kornev N. V., Hassel E., Chorny A. D. Mixing of confined co-axial flows // Int. J. Heat and Mass Transfer. 2006. Vol. 49. P. 3942–3956.
9. Henzler H. J. Investigations on Mixing Fluids. Doctor's Dissertation. Aachen: RWTH, 1978.
10. Becker H. A., Hottel H. C., Williams G. C. Mixing and Flow in Ducted Turbulent Jets // Proc. 9th Symp. (Int.) on Comb. London: Academic Press, 1963. P. 7–20.
11. Barchilon M., Curtet R. Some Details of the Structure of an Axis-Symmetrical Confined Jet with Backflow // J. Basic Eng. 1964. No. 12. P. 777–787.
12. Pope S. B. An Explanation of the Turbulent Round-Jet/Plane-Jet Anomaly // AIAA J. 1978. Vol. 16. No. 3. P. 279–281.
13. Luppes R. The Numerical Simulation of Turbulent Jets and Diffusion Flames // PhD Thesis. Eindhoven: Technische Universiteit, 2000.
14. Lockwood F. C., Stokalis P. Assessment of Two Turbulence Models for Turbulent Round Diffusion Jets with Combustion // Turbulent Shear Flows. Berlin: Springer-Verlag, 1983. Vol. 4. P. 328–328.
15. Abramovich G. N. Theory of Turbulent Jets. Cambridge, MA: MIT Press, 1963.
16. Chorny A. D. Numerical modeling of interaction between a turbulent jet and a co-flow in the cylindrical channel // Reports of the National Academy of Sciences of Belarus. 2007. Vol. 51. No. 1. P. 104–110.
17. Liu Y., Fox R. O. CFD Predictions for Chemical Processing in a Confined Impinging-Jets Reactor // AIChE J. 2005. Vol. 52. No 2. P. 731–744.
18. Chidambaram N., Dash S. M., Kenzakowski D. C. Scalar Variance Transport in the Turbulence Modeling of Propulsive Jets // J. Propulsion and Power. 2001. Vol. 17. No. 1. P. 79–84.
19. Nagano Y., Kim C. A Two-Equation Model for Heat Transport in Wall Turbulent Shear Flows // J. Heat Transfe. 1988. Vol. 110. P. 583–589.
20. Tkatchenko I., Kornev N., Jahnke S., Steffen G., Hassel E. Performances of LES and RANS Models for Simulation of Complex Flows in a Coaxial Jet Mixer // Flow, Turbulence and Combustion. 2007. Vol. 78. No. 2. P. 111–127.

Andrei Chorny

KLAMPAUS NESUSPAUDŽIAMO SKYSČIO APRIBOTOS SROVĖS TURBULENTINIO SUSIMAIŠYMO SKAITINIS MODELIAVIMAS

Santrauka

Straipsnyje pateikiami ašinės srovės ir pasrovio nesuspaudžiamo skysčio srauto modeliavimo ašiniame maišytuve RANS metodu rezultatai. Analizuojami du skirtingi maišymosi režimai – kai susiformuoja recirkuliacinė zona prie maišytuvo sienelių ir kai jos nėra. Palyginti modeliavimo ir eksperimentiniai rezultatai.

Raktažodžiai: srovinis maišytuvas, turbulentinis maišymas, apribotoji srovė, mišinio koeficientas

Андрей Чорный

ЧИСЛЕННОЕ МОДЕЛИРОВАНИЕ ТУРБУЛЕНТНОГО СМЕШЕНИЯ ОГРАНИЧЕННОЙ СТРУИ НЕСЖИМАЕМОЙ ВЯЗКОЙ ЖИДКОСТИ

Резюме

Представлены результаты RANS моделирования взаимодействия турбулентной осесимметричной струи и спутного потока несжимаемой жидкости (число Шмидта $Sc \approx 1000$) в осесимметричном струйном смесителе. Два различных режима смешения анализировались – с образованием рециркуляционной зоны у стенок смесителя и без нее. Верификация известных и разработанных в работе моделей смешения основана на сравнении с имеющимися экспериментальными результатами и данными, полученными с помощью метода крупных вихрей (LES). Результаты показали, что изменение осредненного значения коэффициента смеси и его дисперсии, полученное с привлечением разработанной модели смешения с учетом существования областей потока с низкими турбулентными числами Рейнольдса Re_t (отношение турбулентных масштабов времени пульсаций скорости и концентрации R и турбулентное число Шмидта являются функциями числа Рейнольдса Re_t), подобно LES данным и экспериментальным результатам.

Ключевые слова: струйный смеситель, турбулентное смешение, ограниченная струя, спутный поток, коэффициент смеси